Relaxation of the CH_2 Stretching Modes of Liquid Dihalomethanes

G. Seifert*, M. Bartel and H. Graener

Physics Institute, Martin-Luther-University Halle-Wittenberg, D-06099 Halle, Germany

Abstract: The vibrational relaxation of the liquid dihalomethanes CH_2I_2, CH_2Br_2 and CH_2Cl_2 has been studied by a combination of IR/IR and IR/Raman pump-probe techniques applying a time resolution of ~2 ps. Careful analysis of the results shows a general trend of decreasing relaxation rates from dichloromethane to diiodomethane, with few individual deviations. Possible explanations for these observations are discussed.

1. INTRODUCTION

Liquids composed of small polyatomic molecules are model systems to study the elementary processes of relaxation and dissipation of excess energy. Due to the well-separated vibrational resonances of weakly interacting systems like, e.g., methane derivates, ultrafast pump-probe techniques based on infrared absorption and / or Raman scattering often have the potential to provide a comprehensive picture of individual relaxation channels and the corresponding rates in these systems, when both temporal and spectral information are analyzed [1-5]. The usually complementary nature of Raman and infrared activity of molecular vibrations necessitates to conduct investigations of this type with a combination of both experimental techniques [6]. Such a combined approach provides additional information: anti-Stokes Raman data allow direct access to vibrational excess population, the knowledge about which can then be used to assign excited state transitions seen in the transient IR spectra. The obtained anharmonic shifts are an important piece of information about molecular potentials, Furthermore, these spectral assignments allow to analyze the relaxation dynamics also of Raman-inactive vibrations, and thus in the best case to achieve a comprehensive, self-consistent picture of energy relaxation pathways and rates.

In this work, we focus on the C-H stretching relaxation of three dihalomethanes with increasing molecular weight of the halogen atoms. Though there have been already several ultrafast studies on these molecules, mostly on liquid mixtures [7-13], a comprehensive picture of their vibrational dynamics after C-H stretch excitation disentangling the individual relaxation rates of symmetric and antisymmetric CH stretching vibration has so far not been published.

2. EXPERIMENTAL

The samples studied were the pure liquids CH_2I_2, CH_2Br_2 and CH_2Cl_2 (purity 99% or better) as purchased from Sigma-Aldrich without further purification. IR absorption spectra and stationary Raman spectra of the samples have been recorded with a Bruker Tensor 37 FTIR and a Bruker IFS 66 FT-Raman spectrometer.

Two setups for picosecond time-resolved spectroscopy were used: (i) the first one is an IR pump-probe setup applying two separately tunable, linearly polarized pulses of 2.5 ps duration. As described previously [14, 15] the tuning range is 2.5 μm to ≈ 7 μm for the pump, and 2.5 μm – 10 μm for the probe pulses. In this work we only use the 'magic-angle' signal $\Delta\alpha_{rf}$ defined by $\Delta\alpha_{rf} = \ln(T/T_0)_{\parallel} + 2\cdot\ln(T/T_0)_{\perp}$, where T_0 is the intensity transmission of the sample (without excitation), and $T_{\parallel}$ and $T_{\perp}$ are the transmissions after excitation measured with probe polarization parallel or orthogonal with respect to the pump polarization. (ii) The second system for observation of spontaneous Raman scattering after IR excitation has a pump path identical with system (i), while the (visible) probe pulses in this case have a fixed wavelength of 523.5 nm. The scattered Raman photons are collected and spectrally analyzed with a highly sensitive CCD camera behind a monochromator. Details of the setup have been described previously [3, 6].

In both systems a strong IR pump pulse creates a non-negligible amount of population on a certain vibrational mode, the decay of which is then monitored as a function of the pump-probe delay time by (i) measuring IR absorption changes, or (ii) collecting the Anti-Stokes photons. The latter can be normalized by the Stokes-side data giving the excess vibrational population Δn, which can be quantitatively compared with numerical simulations of Δn. Due to the complementary character of infrared and Raman activity (e.g., the strongly different Raman cross sections of symmetric and antisymmetric CH stretching mode of the liquids studied here), often only a combination of the two techniques yields the comprehensive information.

The IR/IR system (i) was also used in a special mode to study the low-frequency spectra of the liquids: by tuning the excitation wavelength far away from any resonance, and varying the probe wavelength at maximum temporal overlap of pump and probe, Stimulated Raman Gain (SRG) spectra are obtained. These can be converted to a reduced Raman spectrum [16] providing information about the distribution of non-vibrational modes (instantaneous normal modes) of the liquid under consideration. This information will be used in the discussion section.

*Address correspondence to this author at the Universität Halle, Institut für Physik, FG Optik, Hoher Weg 8, D-06099 Halle (Saale), Germany; Tel: +49 345 5525311; Fax: +49 345 5527221;
E-mail: gerhard.seifert@physik.uni-halle.de

1874-0677/08

3. RESULTS

3.1. Stationary Spectroscopy

Before doing ultrafast time-resolved experiments, it is always necessary to first gather any accessible information from conventional spectroscopy, such as band positions, widths or interaction cross sections. For this purpose we have recorded IR and Raman spectra of all three dihalomethanes.

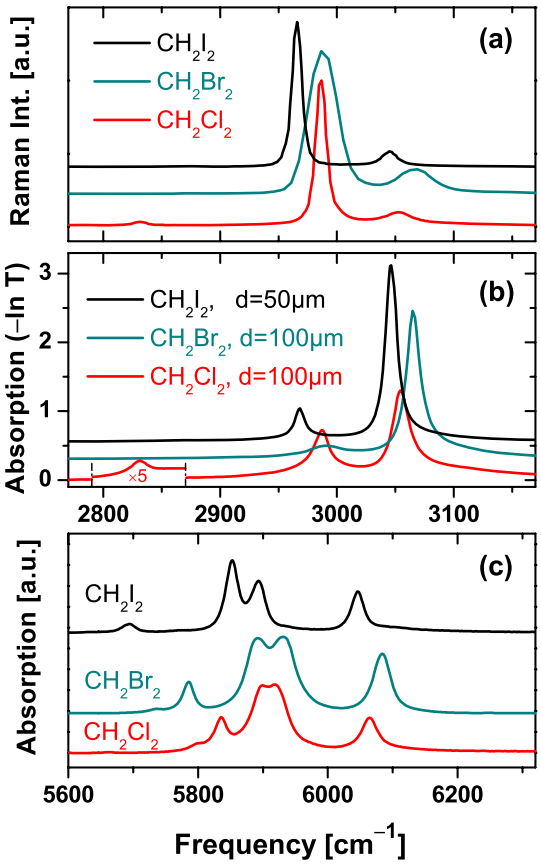

Fig. (1). Vibrational spectra of CH_2I_2 (black), CH_2Br_2 (dark green) and CH_2Cl_2 (red); (a) Stokes Raman (b) IR absorption, CH stretch fundamental region, (c) IR overtone region.

In Fig. (**1**) the C-H stretching regions of the two types of spectra (Fig. (**1a**): Raman, Fig. (**1b**): infrared absorption) are compared: the black curves refer to CH_2I_2, dark green curves to CH_2Br_2, and the red lines represent CH_2Cl_2. The corresponding IR peak frequencies are given in Table **1**. For all three substances the antisymmetric CH_2 stretching mode ν_6 (around 3050cm^{-1}) shows a rather weak Raman signal, but strong IR absorption, and vice versa for the symmetric mode ν_1. The generally low Raman cross section of ν_6 (compare Fig. **1**) causes a limited accuracy of the transient Anti-Stokes scattering signal from this mode in our experiment. At this point our complementary experimental approach for probing the vibrational population with both techniques helps to improve the data accuracy. On the other hand the low ν_1 IR absorption, in particular in the case of CH_2Br_2 where it is a factor of 10 below that of ν_6, makes it difficult to achieve significant transient population of the symmetric C-H stretch. It should be noted that the ν_1 Raman band of CH_2Br_2 is significantly broader than that of the other two liquids.

In transient experiments vibrational population can be observed with Anti-Stokes photons directly at the fundamental frequency, while IR probing has to be done at a hot band frequency in order to avoid ground state depletion being mixed into the signal [6]. The spectral positions of hot bands can, under normal circumstances, be derived from the overtone spectral region. Fig. (**1c**) presents the interesting spectral range where all possible transitions leading to simultaneous excitation of two C-H vibrational stretching quanta are expected.

Table 1. CH_2 Stretching Fundamental and Overtone Frequencies and Anharmonic Shifts of CH_2I_2, CH_2Br_2 and CH_2Cl_2

	CH_2I_2	CH_2Br_2	CH_2Cl_2
ν_1	2968	2984	2984
ν_6	3047	3065	3056
$\nu_1+\nu_6$	5852	5890	5924
$\Delta\nu_{16}$	–163	–158	–143
$2\nu_1$	5893	5932	5895
$\Delta\nu_{11}$	–43	–38	–44
$2\nu_6$	6047	6084	6063
$\Delta\nu_{66}$	–47	–46	–47

For all three liquids the spectra have a similar structure: starting from high frequencies, there is a first peak around 6050 cm^{-1}, followed by a double peak around 5900 cm^{-1}, and finally an additional, weaker absorption band on the low-frequency side. Considering that overtones are usually red-shifted, the peaks around 6050 cm^{-1} can unambiguously be assigned to the $2\nu_6$ mode. For the double peak we ascribe, in analogy to previous work on water molecules (where the combination of the OH stretching modes has the largest anharmonicity [17]), the mode at higher frequency to $2\nu_1$, and the other one to (ν_1 + ν_6). These assignments and the corresponding anharmonic shifts, as given in Table **1**, are compatible to transient IR data, as will be shown below.

3.2. Transient Spectroscopy

We will now present picosecond results and derive the vibrational dynamics of the C-H stretching modes of all three dihalomethanes. We start with an example for the anti-Stokes scattering from a sample of CH_2I_2 as a function of pump-probe delay time, after IR excitation of the antisymmetric C-H_2 stretching mode at 3047 cm^{-1}, shown in a 3-dimensional plot in Fig. (**2**).

The number of Anti-Stokes photons monitored at a frequency shift of 3047 cm^{-1} rises quickly to a maximum at delay zero, then decays more slowly. At the position of the symmetric mode ν_1, also Anti-Stokes intensity is observed, which proves coupling of the two modes. The clearly different peak intensities reflect the different Raman cross sections. The signal at ν_1 rises more slowly, indicating a finite time for the energy transfer between antisymmetric and symmetric CH_2 stretching mode, and then decays typically on the same time scale as ν_6.

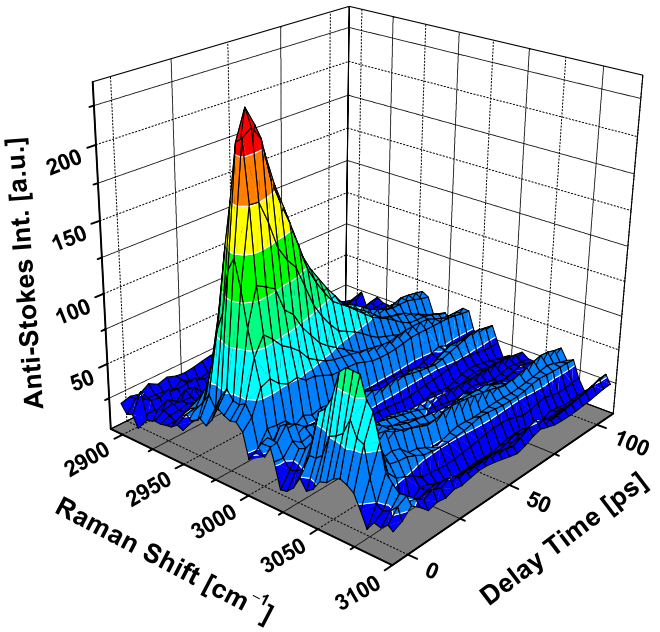

Fig. (2). Transient Anti-Stokes Raman spectra of CH_2I_2 as a function of pump-probe delay time; IR excitation at 3047 cm^{-1} (ν_6).

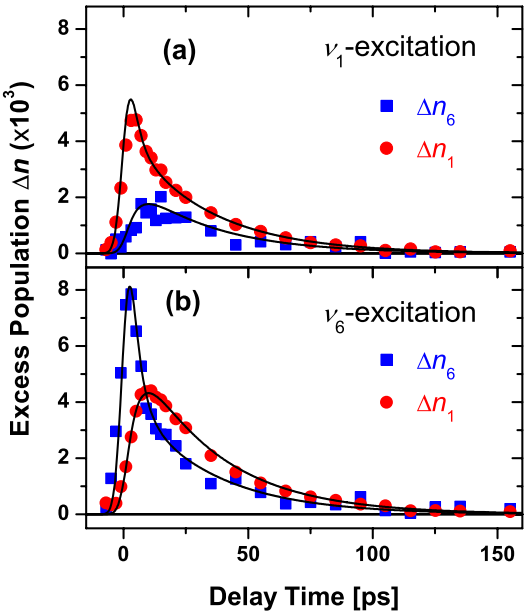

Fig. (3). Transient Anti-Stokes Raman data of CH_2I_2 normalized to relative population.

To analyze the vibrational dynamics in detail, we have derived the relative excess population Δn_i (referring to vibrational level *i*) from the transient anti-Stokes Raman signals obtained by our spectroscopy. For this purpose, the observed bands are spectrally integrated for each delay position and then normalized by help of the Stokes side Raman data [3]. The resulting excess population of CH_2I_2 is plotted as function of delay time in Fig. (**3**). Fig. (**3a**) refers to ν_1, Fig. (**3b**) to ν_6 excitation (same data as in Fig. **2**). Clearly in both cases the excess population of the excited mode reaches its maximum first, while the other vibration is populated with a delay of several picoseconds. Later on, the population of both modes decays with similar time constants.

To analyze these phenomena quantitatively, we have applied a rate equation model [3, 18] composed of ground state, the two CH stretching modes and an intermediate level. Relaxation channels considered were (i) redistribution among ν_1 and ν_6 with time constants τ_{61} and τ_{16} (differing by a Boltzmann factor for detailed balance), and (ii) downward relaxation channels starting from ν_1 and ν_6. Their decay times are denominated by $\tau_{1,\mathrm{eff}}$ and $\tau_{6,\mathrm{eff}}$, indicating that they are effective time constants comprising all contributing physical channels to lower-lying modes.

The black solid lines in Fig. (**3**) are the result of a least mean squares fit based on that rate equation model. Fitting all four curves simultaneously with the same set of parameters, the self-consistent best fit was obtained with the time constants $\tau_{1,\mathrm{eff}}$ = 41 ps, $\tau_{6,\mathrm{eff}}$ = 25 ps, and τ_{61} = 8 ps. This means that in diiodomethane the redistribution among the CH stretching ensemble is significantly faster than the relaxation into lower levels, leading to rather high population also on the unpumped mode (up to 50% of the population on the excited mode). It should be mentioned that the absolute amplitudes (excess population Δn) are the crucial information to sort out in detail the individual values of $\tau_{1,\mathrm{eff}}$ and $\tau_{6,\mathrm{eff}}$.

We have conducted series of comparable experiments also on the other two liquids, CH_2Br_2 and CH_2Cl_2, and subjected these data to the same evaluation and fitting procedure. The resulting relaxation times, summarized in Table **2**, allow two general statements: (i) the vibrational lifetime of the symmetric CH stretching mode is larger than that of the antisymmetric one, and (ii) there is a clear trend to faster vibrational relaxation from CH_2I_2 to CH_2Cl_2, i.e. from heavier to lighter molecules. For CH_2Br_2, however, the ν_1 lifetime is considerably shorter than for the other liquids, and - in particular - has almost the same relaxation rate as the antisymmetric mode.

Table 2. CH_2 Stretching Overtone Frequencies and Anharmonic Shifts of CH_2I_2, CH_2Br_2 and CH_2Cl_2

	CH_2I_2	CH_2Br_2	CH_2Cl_2
$\tau_{1,\mathrm{eff}}$ (ps)	(41 ± 2)	(10 ± 1)	(21 ± 2)
$\tau_{6,\mathrm{eff}}$ (ps)	(25 ± 2)	(9 ± 1)	(5 ± 1)
τ_{61} (ps)	(8 ± 1)	(8 ± 1)	(6 ± 1)

It should be mentioned that our Anti-Stokes Raman data also include lower-lying vibrational modes. For instance, excess population of the C-H bending mode ν_2 is observed for all three liquids in the course of energy relaxation, typically rising with the same time constant as the stretching modes decay. As several other modes can not be analyzed due to their very low Raman cross section, we could not elucidate the relaxation scheme of any of the three substances comprehensively, and therefore restrict this letter to the OH stretching modes. Based on the knowledge of their dynamics gained from the IR pump / Raman probe experiments, we will now analyze in detail time resolved IR / IR experiments on the same samples. Main goals will be (i) to get additional information about molecular anharmonicity, and (ii) confir-

mation or improved precision for the obtained relaxation rates.

Let us first have a look at transient IR spectra obtained on a sample of CH_2I_2, as shown in Fig. (**4**). Since bleaching of the fundamental bands involves also ground state depletion in the IR case, a signal directly proportional to excess vibrational population is found only at the positions of hot bands. In Fig. (**4**) only the region of induced absorptions starting from ν_1 or ν_6, i.e. frequencies below 3020 cm^{-1}, is shown. Comparing the three spectra measured at increasing delay times of 0, 5, and 20 ps, one recognizes at least 4 bands of induced absorption at 2997, 2927, 2884 and 2810 cm^{-1}; additionally one region of slight bleaching (positive $\Delta\alpha_{rf}$) is seen around the position of the ν_1 fundamental at ~2967 cm^{-1}. We can now use our knowledge of the vibrational dynamics for an assignment of the observed hot bands: since ν_6 was pumped for the data in Fig. (**4**), the population of this mode has its maximum around zero delay (maximum temporal overlap of pump and probe), and then decays exponentially; ν_1 is populated indirectly *via* coupling to ν_6 and therefore reaches a maximum some picoseconds later, before it decays also with a similar time constant as ν_6. Accordingly, ν_6 population is monitored at 2810 and 2997 cm^{-1}, whereas at 2884 and 2927 cm^{-1} the delayed maximum of the signals clearly indicates ν_1 dynamics. Without any doubt we observe the transition $\nu_6 \rightarrow 2\nu_6$ at 2997 cm^{-1}. The other ν_6–type dynamics at 2810 cm^{-1} thus belongs to the $\nu_6 \rightarrow \nu_1 + \nu_6$ transition. Considering the necessarily constant anharmonic shift of the combination mode, we can finally assign the induced absorption at 2887 cm^{-1} to the transition $\nu_1 \rightarrow \nu_1 + \nu_6$, and the one at 2927 cm^{-1} to $\nu_1 \rightarrow 2\nu_1$. The additional induced absorption indicated above 3020 cm^{-1} at later delay times (blue curve) is due to population on a lower vibrational level, most probably the C-H bending mode ν_2.

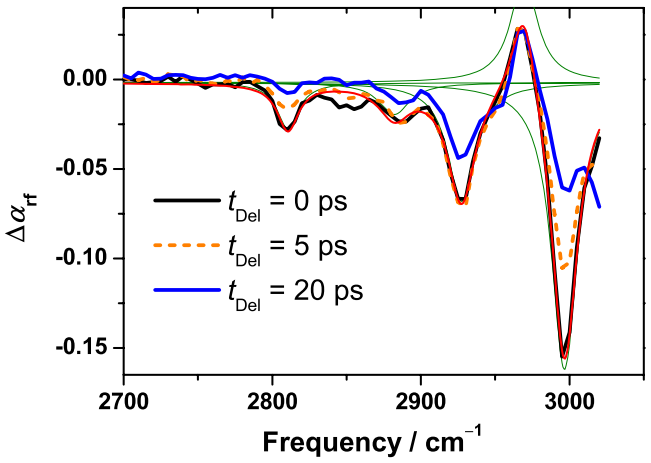

Fig. (4). Transient IR spectra of CH_2I_2 after excitation at 3047cm^{-1} (ν_6).

A reliable assignment must be compatible to the overtone spectra (Fig. **2**). Analyzing the transient data of CH_2I_2 yields $\Delta\nu_{16}$ = (−158 ± 5) cm^{-1}, $\Delta\nu_{11}$ = (−41 ± 3) cm^{-1}, and $\Delta\nu_{66}$ = (−49 ± 3) cm^{-1}. This is, within experimental accuracy, perfectly in accordance with the conventional IR results (compare Table **1**). In other words, all four possible transitions from fundamental C-H stretching modes to second-order combination tones have been identified. It should be noted that the amplitudes of the transitions to ($\nu_1 + \nu_6$) are considerably smaller than those of the overtone transitions. The only spectral change without assignment so far is the weak induced absorption around 2850 cm^{-1}. The temporal behavior of this effect suggests that it represents a transition starting from ν_6, and ending at a third-order combination level. Since this transition is not needed for the interpretation of our data, we do not want to speculate about that mode.

Similar data have been recorded for the other two liquids CH_2Br_2 and CH_2Cl_2: Fig. (**5**) shows transient spectra for methylene bromide at the delay times 2, 6 and 20 ps (lower panel), and one example at the delay time 2 ps for methylene chloride (upper panel). Comparing the spectra from the two liquids measured at t_{Del} = 2ps (in both cases the maximum of observed transmission changes), one recognizes a striking difference: while for CH_2Cl_2 bleaching of both C-H stretch fundamentals and two ranges of induced absorption are observed, CH_2Br_2 exhibits more or less only bleaching of the antisymmetric stretch and the corresponding excited state absorption (at ~3012 cm^{-1}). There is only a very weak indication of transmission changes connected with ν_1 population of CH_2Br_2; vertical lines in the Figure indicate the expected positions of bleaching (solid line) and induced absorption (dash-dotted). Also the later delay times shown do not bring up any additional effects in the spectral range below 3000 cm^{-1}. There is, however, similar to CH_2I_2 a delayed component of induced absorption occurring at ~3045cm^{-1}, as is clearly visible at t_{Del} = 20ps. Analogous to diiodomethane, this contribution can be attributed to a transition starting from lower vibrational modes (e.g., ν_2), which are being populated in the course of C-H stretch energy relaxation.

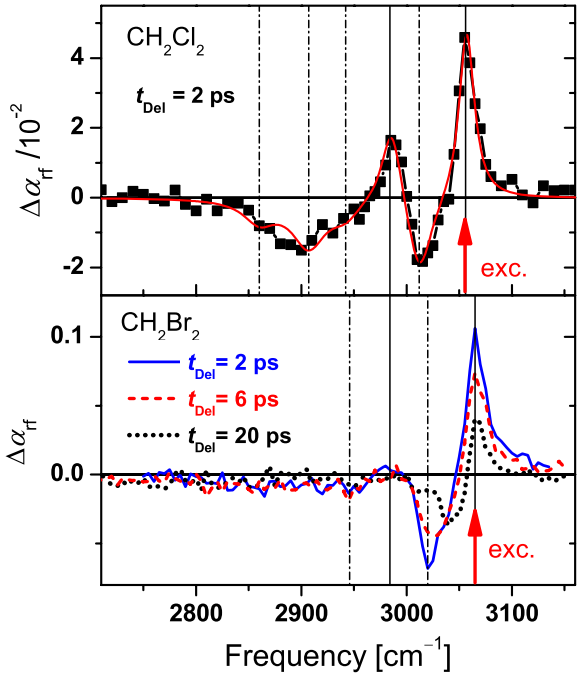

Fig. (5). Transient IR spectra of CH_2Cl_2 and CH_2Br_2 after ν_6 excitation (3056 or 3065 cm^{-1}, respectively).

The observed lack of significant transient spectral changes due to ν_1 population in the case of CH_2Br_2 can apparently be explained by the very low absorption cross section for this mode derived from conventional IR spectra (less than

10% of ν_6, see Fig. **1b**). In contrast, the two C-H stretching mode absorptions of CH_2Cl_2 are differing by less than a factor of 2 only, and consequently transient spectral changes connected with both modes can be observed. Therefore, an overtone analysis like in the case of CH_2I_2 can be done: the solid red line in Fig. (**5**) represents a simulated spectrum composed of 6 Lorentzian bands assigned to bleaching of the two fundamentals (positions indicated by solid vertical lines) and the 4 aforementioned induced absorptions due to transitions starting from ν_1 or ν_6. While the positions of fundamental bleaching and the associated overtone transitions $\nu_{1,6} \rightarrow 2\nu_{1,6}$ are perfectly compatible with the conventional overtone spectra (see Fig. (**2b**) and Table **1**), the anticipated transitions to $\nu_1 + \nu_6$ required slightly deviating anharmonic shifts of 127 and 149 cm^{-1} for a reasonable agreement with the experimental data. A first idea to explain this effect comes from the conventional IR spectrum: the red solid curve in Fig. (**1b**) shows, with amplitude enlarged by a factor of 5, a weak absorption at 2831 cm^{-1}, which can be attributed to the C-H bending overtone $2\nu_2$. Previous experiments [19] and the analogy to H_2O molecules [5] suggest that this mode becomes populated during CH stretch relaxation. If this assumption is true, the corresponding bleaching of $2\nu_2$ might compensate the transition $\nu_6 \rightarrow \nu_1 + \nu_6$, which is actually expected at 2833 cm^{-1} ($\Delta\nu_{16} = -143$ cm^{-1}, compare Table **1**). Further experiments with improved signal-to-noise ratio will be necessary to clear this question.

Comparing the induced absorptions of all three liquids, an interesting general conclusion can be drawn: the relative amplitudes of transitions to the combination mode $\nu_1 + \nu_6$ are small for CH_2I_2, very small for CH_2Br_2 and rather strong for CH_2Cl_2. This behavior appears to be correlated to the balance of the absorption cross sections of ν_1 and ν_6, which differ most for CH_2Br_2, whereas the roughly equal oscillator strengths in the case of CH_2Cl_2 obviously provide a transition dipole to the combination mode being comparable to that created by the much stronger C-H stretch absorptions of CH_2I_2.

Finally, various time resolved IR/IR data have also been recorded and fitted by numerical simulations based on the same rate equation model as the anti-Stokes Raman results. Considering only spectral positions where the above overtone analysis yielded an unambiguous assignment, it was possible to find a self-consistent set of time constants for each liquid. The results obtained by this procedure fully confirmed the time constants given in Table **2**. It is quite interesting to note that the abovementioned comparably fast relaxation of CH_2Br_2 coincides with the special situation of a very low ν_1 absorption cross section and the apparent absence of a transition to the C-H stretch combination mode.

DISCUSSION

We start the discussion of the results with the observed general trend that energy relaxation is accelerated when the molecular weight of the halogen atoms in the three studied dihalomethanes is decreased. The relaxation rate of a populated vibrational mode *j* can, in a very general formulation of Fermi's golden rule, be given as

$$k_j \propto \sum_f \left|\langle \sigma_f \left| V_{if} \right| \sigma_i \rangle\right|^2 P_{bath}\left(\Delta E_{if}\right) \quad (1)$$

Here, V_{if} is the interaction potential enabling a transition from initial (σ_i) to final (σ_f) state of the excited molecule under consideration. P_{bath} comprises the probability of transferring the energy mismatch ΔE_{if} between initial and final state to the thermal bath. In general, equation (1) is a sum over many independent possible channels for energy relaxation. Depending on the number of vibrational (accepting) modes σ_f of the molecules, there are two limiting cases: (i) There are so many vibrational levels in close energetic proximity to the initial state σ_i that only a small ΔE_{if} has to be transferred to the thermal bath and an intramolecular relaxation of the vibrational energy happens; this is typically the case for large molecules providing a density of at least 10 vibrational states per cm^{-1} around the excited mode [20]. (ii) The other limit is that there are only a few acceptor levels in the interesting energy region, and a single pathway with large transition dipole element and non-negligible ΔE_{if} (typically 10 to 100cm^{-1}) is dominating the relaxation, which may be intra- or intermolecular. In that case, the magnitude of the energy mismatch and/or the density of thermal bath modes (in the instantaneous normal mode picture) available at the needed ΔE_{if} are often crucial for the observed relaxation rates. In contrast, in the first case the density of accepting modes is the decisive parameter which can often directly be correlated to different relaxation rates of otherwise similar molecular systems.

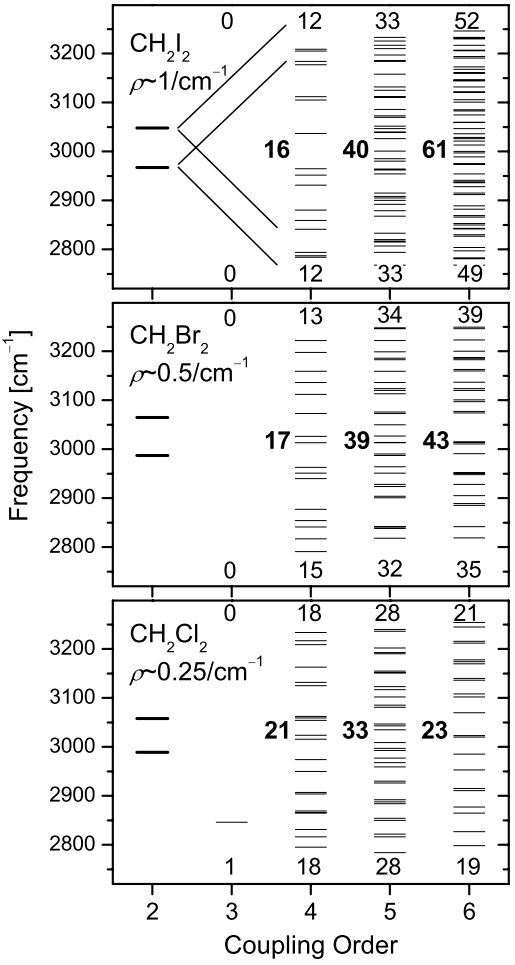

Fig. (6). States within 200 cm^{-1} of the C-H stretching modes of the three studied dihalomethanes as a function of coupling order (for definition see text).

We now want to test which of the two limiting cases sketched above is more appropriate for the dihalomethanes. For this, we analyze the accepting modes of the three dihalomethanes in harmonic approximation. Fig. (**6**) gives the available levels in an interval of 200 cm^{-1} above ν_6 and below ν_1, respectively. This interval was selected with respect to the low-frequency spectra of the liquids (see below), which suggest considerable density of modes of the thermal bath only below this energy limit. In Fig. (**6**), only the states from 3rd to 6th coupling order (total change in the number of quanta) in this interval are shown. The numbers refer to the number of modes of the respective coupling order in the interval [$\nu_6 \pm 200cm^{-1}$] (top of each panel), [$\nu_1 \pm 200cm^{-1}$] (bottom), and [$\nu_1 - 200cm^{-1}$ … $\nu_6 + 200cm^{-1}$] (center). We also calculated the total number of states in the latter interval and converted it to an average density of states ρ, also given in the Figure. From this value one can clearly see that we are not in the limiting case (i) where only the number of accepting modes is the crucial parameter, because the density of available states suggests just the opposite trend for the relaxation rates as was observed.

A more convenient picture is obtained from the 3rd and 4th order coupling states alone: their number increases along with the observed increase of relaxation rates, and in particular a state ($2\nu_2$) is available by 3rd order coupling in the case of CH_2Cl_2, which experimentally exhibited the fastest relaxation (τ_{6eff} = 5ps). There is, however, no simple argument why ν_6 should be relaxing faster then ν_1: the number of accepting modes by 4th order coupling (and higher) is practically equal in all cases, and the only 3rd order coupling state available in the case of CH_2Cl_2 is energetically closer to ν_1. We may therefore conclude that, like in the case of haloform molecules, vibrational energy relaxation of the C-H stretch modes of dihalomethanes is controlled by a few specific channels [21-23], and thus the observed relaxation rates will depend on the individual transition dipole moments and the available bath modes.

To learn more about the low-frequency modes, we have used our IR pump-probe setup to measure spectra of stimulated Raman gain. Tuning the pump pulse to a frequency in the transparent region of the sample (here 3300cm^{-1}), a temporally overlapping probe pulse experiences Raman gain (loss) at negative (positive) frequency difference $\Delta\nu = \nu - \nu_{Pu}$. This signal can be converted to a reduced Raman spectrum $R(\nu)$, which is a direct measure of the spectral distribution of bath modes [16], weighted by their intermolecular polarizability.

The solid lines in Fig. (**7**) have been calculated as guide to the eye. In order to conveniently extract the characteristic parameters of the three spectra, we calculated the first and second spectral moments of the range shown in Fig. (**7**). The result, given in the order CH_2I_2, CH_2Br_2, and CH_2Cl_2 is: maximum ('center of gravity') at 34 cm^{-1}, 46 cm^{-1} and 57 cm^{-1}; width of distribution: 32 cm^{-1}, 48 cm^{-1}, and 52 cm^{-1}. This confirms the visual impression that the low-frequency spectra stretch out to higher frequencies with decreasing molecular weight of the dihalomethanes. Thus, larger energy mismatches ΔE_{if} can be accepted or provided by the thermal bath of the lighter dihalomethane molecules. This is on the one hand nicely in accordance with the observed general trend of C-H stretch relaxation, but can, on the other hand, by no means explain the individual differences of the C-H stretching modes. It is, for instance, unclear why the relaxation rates of ν_1 and ν_6 are nearly equal for CH_2Br_2, but differ by more than a factor of 4 in the case of CH_2Cl_2.

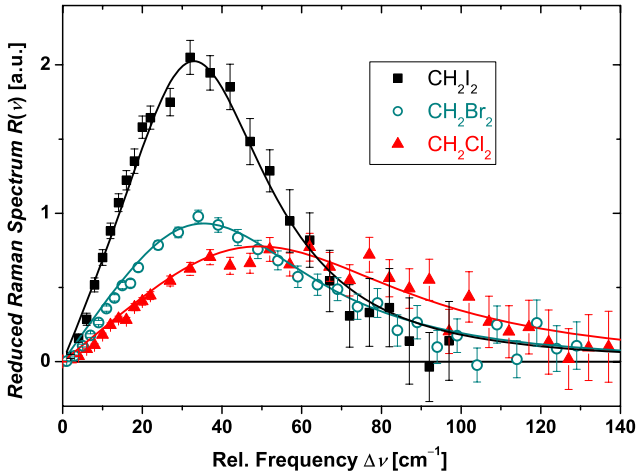

Fig. (7). Reduced Raman spectra of CH_2I_2, CH_2Br_2, and CH_2Cl_2.

Searching for additional arguments in this context, some rather old work is noteworthy: by analyzing the solvent dependence of C-H_2 stretching band intensities of methylene halides, Evans and Lo [24] found more than 40 years ago that the C-H dipole derivatives of these molecules are very sensitive to solute-solvent interaction, which was interpreted as to be caused by an (intramolecular) charge transfer upon formation of a (weak) hydrogen bond. We checked this effect for our substances and found that, e.g., upon dilution of 1:100 in the inert solvent CCl_4 the ratio of peak absorbances $A(\nu_1)/A(\nu_6)$ changes from 0.56 to 2.66 for CH_2Cl_2, and from 0.088 to 0.20 for CH_2Br_2. So obviously the intermolecular interactions in the neat liquids are strong enough to considerably modify the molecular dipoles, and it appears straightforward to expect also a considerable influence on the interaction potential V_{if} (see eq. (1)). So the comparably fast ν_1 relaxation of CH_2Br_2 might be interaction-induced, if one assumes, e.g., the strongest interaction to be present between CH_2Br_2 molecules.

Another idea, why the symmetric C-H stretching mode of dibromomethane could have the highest relaxation rate, comes from the doublet nature of this mode observed in Raman spectra, at lower spectral resolution like in Fig. (**1**) only seen as broadening. The splitting of this band has been explained by Fermi resonance to a close-lying combination mode; different authors suggested different resonant levels like $\nu_2 + 2\nu_7$ [24, 25], $2\nu_3 + \nu_8 + \nu_9$ [26, 27], or $\nu_2 + 2\nu_4 + 2\nu_9$ [25]. Irrespective which of those assignments is correct, the strong coupling of the Fermi resonant mode would provide a good explanation for the acceleration of the ν_1 relaxation in the case of CH_2Br_2.

Finally, we want to compare the relaxation rates obtained in this study with individual values reported in previous work. Graener and Laubereau reported (12±2)ps and (7±1)ps for the ν_1 lifetimes of neat CH_2Cl_2 and CH_2Br_2, respectively, and (45±5)ps for a 1:1 volume mixture of CH_2I_2 in CCl_4 [7]. While the first two values are in agreement with the current results (single exponential fits to comparable data yielded

~11ps and ~8ps), the last one differs considerably from the ~32ps, which can be derived from comparable current data on neat CH_2I_2. We tentatively interpret this relaxation rate decrease as solvent effect. Several other studies using pump-probe setups were also conducted on solutions [8-13]. In these studies, often a simplified interpretation approach was used with only one intra- and one intermolecular relaxation rate comprising all possible individual channels. The values obtained in these studies can therefore not directly be compared to, but are fairly compatible with those obtained in this work, at least when the abovementioned solvent effects are being accounted for. We are planning future investigations in a new setup with strongly improved signal-to-noise ratio on dihalomethanes in solution, in order to retrieve the missing steps for comprehensive relaxation schemes, and to learn more about further open questions like the anticipated solvent effects.

CONCLUSIONS

We have investigated the vibrational energy relaxation of three dihalomethanes (CH_2I_2, CH_2Br_2, and CH_2Cl_2.) after C-H stretch excitation with a combined approach of IR/IR and IR/Raman pump probe spectroscopy. A careful analysis of the time-resolved results yielded a detailed picture of the coupling of symmetric (ν_1) and antisymmetric (ν_6) mode and their individual relaxation rates to lower-lying states. Internal redistribution among ν_1 and ν_6 as well as the relaxation rate of ν_6 show a general trend to acceleration of the dynamics from dichloromethane to diiodomethane, which is correlated with the increasing molecular weight of the halogen atoms. The symmetric C-H_2 stretch, having the longest lifetime for all three substances, deviates from this rule, exhibiting the fastest dynamics for CH_2Br_2 (decay time 10 ps). Possible explanations for this peculiarity of CH_2Br_2 are (i) interaction-induced modification of the respective transition dipole leading to very low IR absorption of ν_1, or (ii) Fermi resonance of ν_1 to a nearby combination mode, causing a doublet structure visible in the Raman spectrum. The low ν_1 IR cross section of CH_2Br_2 also prohibited an overtone assignment from transient IR spectra, which in contrast worked well for the other two liquids.

Currently we are reconfiguring our setup to achieve significantly higher experimental accuracy. This will open the perspective to study especially the influence of solute-solvent interaction on the vibrational dynamics by investigating dihalomethanes at low concentration in binary mixtures.

Received: June 13, 2008 Revised: Novembre 10, 2008 Accepted: November 11, 2008

ACKNOWLEDGEMENT

The authors are grateful to I. Otten for conventional spectra and to S. Thränert for part of the transient IR spectra. This work was financially supported by the Deutsche Forschungsgemeinschaft through grant DFG SE986/3-3.

REFERENCES

[1] Deak, J.C.; Iwaki, L.K; Dlott, D.D. *J. Phys. Chem. A*, **1999**, *103*, 971.
[2] Dlott, D.D. *Chem. Phys.*, **2001**, *266*, 149.
[3] Graener, H.; Zürl. R.; Hofmann, M. *J. Phys. Chem.*, **1997**, *101*, 1745.
[4] Seifert, G.; Zürl, R.; Patzlaff, T.; Graener, H. *J. Chem. Phys.*, **2000**, *112*, 6349.
[5] Seifert, G.; Patzlaff, T.; Graener, H. *J. Chem. Phys.*, **2006**, *125*, 154506
[6] Seifert, G.; Zürl, R.; Graener, H. *J. Phys. Chem. A*, **1999**, *103*, 10749.
[7] Graener, H.; Laubereau, A. *Appl. Phys. B*, **1982**, *29*, 213.
[8] Bingemann, D.; King, A.M; Crim, F.F. *J. Chem. Phys.*, **2000**, *113*, 5018.
[9] Heckscher, M.M; Sheps, L.; Bingemann, D.; Crim, F.F. *J. Chem. Phys.*, **2002**, *117*, 8917.
[10] Bakker, H.J.; Planken, P.C.M.; Lagendijk, A. *J. Chem. Phys.*, **1991**, *94*, 6007.
[11] Cheatum, C.M.; Heckscher, M.M.; Bingemann, D.; Crim, F.F. *J. Chem. Phys.*, **2001**, *115*, 7086.
[12] Charvat, A.; Aßmann, J.; Abel, B.; Schwarzer, D.; Henning, K.; Luther, K.; Troe, J. *Phys. Chem. Chem. Phys.*, **2001**, *3*, 2230.
[13] Elles, C.G.; Bingemann, D.; Heckscher, M.M.; Crim, F.F. *J. Chem. Phys.*, **2003**, *118*, 5587.
[14] Graener, H.; Patzlaff, T.; Seifert, G. *Vib. Spectrosc.*, **2000**, *23*, 219.
[15] Graener, H.; Patzlaff, T.; Seifert, G. *Opt. Commun.*, **2002**, *214*, 297.
[16] Seifert, G. *Chem. Phys. Lett.*, **2003**, *370*, 309.
[17] Benedict, W.S; Gailar, N.; Plyler, E.K. *J. Chem. Phys.*, **1956**, *24*, 1139.
[18] Graener, H.; Seifert, G.; Laubereau, A. *Chem. Phys.*, **1993**, *175*, 193.
[19] Hofmann, M.; Graener, H. *Chem. Phys.*, **1996**, *206*, 129.
[20] Yoo, H.S.; DeWitt, M.J.; Pate, B.H. *J. Phys. Chem. A*, **2004**, *108*, 1348.
[21] Sibert III, E.L.; Rey, R. *J. Chem. Phys.*, **2002**, *116*, 237.
[22] Ramesh, S.G.; Sibert III, E.L. *J. Chem. Phys.*, **2006**, *124*, 234501.
[23] Ramesh, S.G.; Sibert III, E.L. *J. Chem. Phys.*, **2006**, *125*, 244512.
[24] Evans, J.C.; Lo, G.Y-S.; *Spectrochim. Acta*, **1965**, *21*, 33.
[25] Fernandez Bertran, J.; La Serna Torres, B.; Fernandez Felix, D. *J. Raman Spectrosc.*, **1988**, *19*, 33.
[26] Fukushi, K.; Kimura, M. *J. Raman Spectrosc.*, **1979**, *8*, 125.
[27] Fernandez Bertran, J. *Spectrochim. Acta A*, **1985**, *41*, 959.